

Cite this: *Chem. Commun.*, 2012, **48**, 7856–7858

www.rsc.org/chemcomm

## COMMUNICATION

## Is a radical bridge a route to strong exchange interactions in lanthanide complexes? A computational examination†

Thayalan Rajeshkumar and Gopalan Rajaraman\*

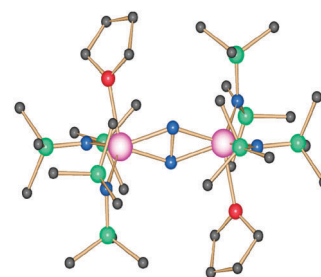
Received 14th May 2012, Accepted 6th June 2012

DOI: 10.1039/c2cc33483f

The origin of very strong antiferromagnetic exchange in  $N_2^{3-}$  bridged complex,  $[[\{(Me_3Si)_2N\}_2Gd(THF)]_2(\mu-\eta^2:\eta^2-N_2)]^-$  (**1**) has been probed using density functional theory (DFT) combined with molecular orbital (MO) and natural bond orbital (NBO) analysis. The analysis helps us to propose a generic mechanism of coupling for a {2p–4f} class of compounds.

The requirement of high anisotropy to enhance the barrier height in Single Molecule Magnets (SMMs)<sup>1,2</sup> has led researchers to focus their attention on the 4f-ion based clusters<sup>3</sup> and their combination with transition metals {3d–4f} or radicals {2p–4f}. This synthetic strategy has tremendous success in producing novel SMMs in a short span of time.<sup>4,5</sup> The 4f-ion based clusters have also yielded several novel SMMs, for example Winpenny *et al.* reported a  $\{Dy^{III}_5\}$  cluster possessing the largest barrier height for any cluster compounds.<sup>6</sup> It is however to be noted that the observed SMM characteristics of these complexes are essentially due to the single-ion anisotropy of  $Dy^{III}$  ions and a primary challenge in such clusters is the very weak exchange interaction leading to close lying excited states and a fast quantum tunnelling of magnetization.<sup>6,7</sup> A recent study on a  $\{Dy^{III}_2\}$  dinuclear complex by Powell *et al.* reveals that the Ising type exchange coupling between the  $Dy^{III}$  ions suppresses the quantum tunnelling of magnetization at zero-field.<sup>8</sup> This emphasises the importance of the exchange interaction in developing new generation SMMs. The {2p–4f} class of compounds, on the other hand, are slightly superior to 4f- and {3d–4f} systems as moderate to strong exchange interactions have been observed in this class of compounds and the magnitude can be tuned at will.<sup>4</sup>

Recently, Long *et al.* reported a new class of  $Gd^{III}$  dimeric complexes containing  $N_2^{3-}$  radical anionic bridging<sup>9</sup>  $[[\{(Me_3Si)_2N\}_2Gd(THF)]_2(\mu-\eta^2:\eta^2-N_2)]^-$  (**1**) and  $N_2^{2-}$  anionic bridging<sup>10</sup>  $[[\{(Me_3Si)_2N\}_2Gd(THF)]_2(\mu-\eta^2:\eta^2-N_2)]$  (**2**) complexes (See Fig. 1). Complex **1** exhibits the strongest antiferromagnetic interaction reported for any 4f- ion based cluster.<sup>3</sup> The  $Gd^{III}$

Fig. 1 Crystal structure of the complex **1**.

and the radical  $N_2^{3-}$  interaction is reported to be  $-27\text{ cm}^{-1}$  (see Table 1). On the other hand, complex **2** exhibits a weak antiferromagnetic exchange between two  $Gd^{III}$  atoms ( $J_{Gd-Gd} = -0.49\text{ cm}^{-1}$ ). Given the importance of achieving large  $J$  values in 4f-ion based clusters and the fact that the  $J$  value of **1** is larger than any {3d–4f} class of compound reported,<sup>5</sup> we were motivated to explore the origin of the magnetic interaction in complex **1**.

Here, we applied DFT methods to compute magnetic exchange interactions in **1** and **2** and performed MO and NBO analysis to gain insight into the mechanism of magnetic coupling. Magneto-structural correlations have also been developed to offer a way to further enhance the  $J$  values in this class of compounds. The  $Gd^{III}$  ions in **1** and **2** are five-coordinate with average Gd–N distances of 2.237 and 2.340 Å, respectively. The bridging N–N distances are distinctly different with a longer N–N (1.40 Å) for **1** and a relatively shorter one for **2** (1.278 Å). The  $\{Gd_2N_2\}$  core lies in a plane with a Gd–N–Gd–N dihedral angle of  $0^\circ$  in both the complexes. For complex **1** the following exchange Hamiltonian has been adopted for the computation of  $J$  values:

$$\hat{H} = -2J_1(\hat{S}_{Gd_A}\hat{S}_{rad} + \hat{S}_{Gd_B}\hat{S}_{rad}) - 2J_2\hat{S}_{Gd_A}\hat{S}_{Gd_B}$$

Here,  $J_1$  describes interactions between  $Gd^{III}$  ions and  $N_2^{3-}$  radicals, while  $J_2$  denotes the Gd–Gd non-neighbour interaction. For complex **2**, only the Gd–Gd interaction is applicable and this has been computed. A pair-wise interaction model has been employed to compute multiple  $J$  values within this cluster (see the ESI for an elaborate discussion†).<sup>11</sup>

The DFT calculations<sup>12</sup> yield  $J_1 = -23.7\text{ cm}^{-1}$  and  $J_2 = -0.53\text{ cm}^{-1}$  for complex **1**. For complex **2**, a  $J_{Gd-Gd}$  interaction of  $-0.51\text{ cm}^{-1}$  has been obtained. A strong antiferromagnetic  $J_1$  in **1** supports experimental observations and the computed magnitude is in good accord with the experimental value

Department of Chemistry, Indian Institute of Technology–Bombay, Powai, Mumbai-400076. E-mail: rajaraman@chem.iitb.ac.in; Tel: +91-22-2576-7187

† Electronic supplementary information (ESI) available: Computational details, computed spin density tables, spin density plots, magnetic orbitals, molecular orbital diagrams, experimental exchange coupling values for some 3d–4f complexes and overlap integral values. See DOI: 10.1039/c2cc33483f

**Table 1** Experimental and DFT computed exchange coupling constants of different Gd<sup>III</sup>-radical complexes reported in the literature

Complexes	$J_{\text{exp}}/\text{cm}^{-1}$	$J_{\text{cal}}/\text{cm}^{-1}$	Ref.
[[{(Me <sub>3</sub> Si) <sub>2</sub> N <sub>2</sub> Gd(THF)} <sub>2</sub> ( $\mu$ - $\eta^2$ : $\eta^2$ -N <sub>2</sub> )] <sup>-</sup> ( <b>1</b> )	-27	-23.7/-0.53	9
[Gd(Hbpz <sub>3</sub> ) <sub>2</sub> (dtbsq)]	-5.7	-6.18	4b
[Gd(NITBzImH) <sub>2</sub> (NO <sub>3</sub> ) <sub>3</sub> ]	-4.05	-2.85	4d
[Gd(NITMeBzImH) <sub>4</sub> ](ClO <sub>4</sub> ) <sub>3</sub>	-3.8	—	4d
[Gd(hfac) <sub>3</sub> (IM <sub>2</sub> py)]	-3	-2.26	4e
[Gd(hfac) <sub>3</sub> (IMBzImH)]	-2.6	—	4c
[Gd(NITBzImH) <sub>4</sub> ](ClO <sub>4</sub> ) <sub>3</sub>	-1.8	-1.28	4d
[Gd(hfac) <sub>3</sub> (imvd)]	-1.58	—	4f
{Gd[(TCNQF <sub>2</sub> ) <sub>2</sub> (H <sub>2</sub> O) <sub>6</sub> ](TCNQF <sub>4</sub> )	-1.4	—	4g
[[{(Me <sub>3</sub> Si) <sub>2</sub> N <sub>2</sub> Gd(THF)} <sub>2</sub> ( $\mu$ - $\eta^2$ : $\eta^2$ -N <sub>2</sub> )]	-0.49	-0.51	10
[Gd(TCNE) <sub>3</sub> ·x(MeCN)]	-0.05	—	4h

(see Table 1). Although the  $J_2$  interaction has not been estimated experimentally for complex **1**, the estimate obtained for **2** serves the purpose of comparison and our calculations reveal that a weak non-neighbour Gd–Gd antiferromagnetic interaction is operational in both the complexes. This set of  $J$  values leads to an  $S = 13/2$  ground state with the  $S = 11/2$  and  $9/2$  excited states at 8.2 and 16.9 cm<sup>-1</sup>, respectively for **1**. We have also extended our studies to other antiferromagnetically coupled Gd<sup>III</sup>-radical systems reported in the literature and this has been done primarily for comparison and also to depict a generalised picture of the coupling mechanism in the {2p–4f} class of compounds. In all the computed cases, the  $J_{\text{cal}}$  is in excellent agreement with the  $J_{\text{exp}}$  reported. From Table 1 it is also clear that the  $J$  value calculated for complex **1** is highest of all the {2p–4f} class of compounds (see ESI, Table S4 for a comparison with other classes of compounds†).

The computed ground state spin density plots for **1** and **2** are shown in Fig. 2a–b. The Gd<sup>III</sup> atoms have a spherical spin distribution, having spin densities of 7.01 and 7.04 for **1** and **2** respectively. The nitrogen atoms of the N<sub>2</sub><sup>3-</sup> bridge in **1** have spin densities of 0.47 and 0.48 and this indicates a near symmetrical distribution of spin densities on both the nitrogen atoms. The magnitude of the spin densities on the nitrogen atoms in **1** is the largest, among the {2p–4f} class of compounds, computed (see Table S2 and S3 and Fig. S1†) revealing a large localization of spin densities on the N<sub>2</sub><sup>3-</sup> moiety. The unpaired electron in the N<sub>2</sub><sup>3-</sup> moiety is found to be located in a  $\pi^*$  orbital ( $\pi_{\text{py}}^*$ ), which is perpendicular to the {Gd<sub>2</sub>N<sub>2</sub>} plane (see Fig. 2a and Fig. S3† for a qualitative MO diagram).

In general, there are two contributions to the magnetic coupling in {2p–4f} based systems, the first one being a direct

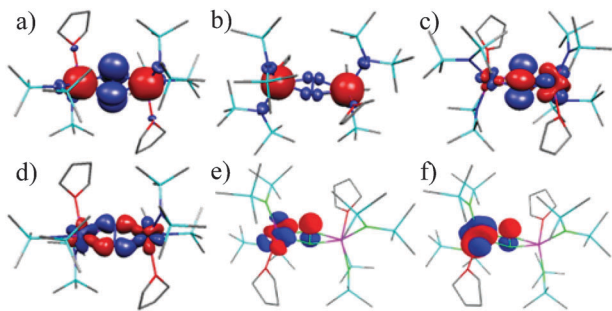


**Fig. 2** High spin (HS) spin density plots of (a) **1** and (b) **2**. Superimposed orbitals for **1**: (c)  $\pi_{\text{py}}^*$  with a 4f orbital of Gd<sup>III</sup>; (d)  $\pi_{\text{py}}^*$  with 4f orbitals of Gd<sup>III</sup>. (e–f) NBO orbitals where significant donor–acceptor stabilisation been detected.

overlap of the 4f- magnetic orbitals with the radical orbital of the N<sub>2</sub><sup>3-</sup> unit. The second is an indirect contribution where partial charge transfer (CT) from N<sub>2</sub><sup>3-</sup> to 5d/6s orbitals of Gd<sup>III</sup> takes places. Here, the former will have both ferromagnetic, as well antiferromagnetic, contributions to the net exchange, while the latter contributes exclusively to the ferromagnetic part of the net exchange.<sup>13</sup> The sign and magnitude of the net exchange interaction is decided by these two competing contributions. Recently, using DFT methods, we have proposed that these two contributions can be qualitatively analysed using computation of overlap integrals  $S_{\text{ab}}$  (direct) between the magnetic orbitals and NBO analysis (indirect). The computed  $S_{\text{ab}}$  values between the Gd<sup>III</sup> 4f-orbitals and the  $\pi_{\text{py}}^*$  orbital of N<sub>2</sub><sup>3-</sup> are given in Table S4.† Interestingly, a significant overlap between the  $\pi_{\text{py}}^*$  orbital of the N<sub>2</sub><sup>3-</sup> moiety and two 4f orbitals of the Gd<sup>III</sup> (see ESI for orbital labels†) has been observed. These two orbitals lobes are aligned with the  $\pi_{\text{py}}^*$  orbital and this essentially leads to a strong overlap (see Fig. 2c). For the Gd··Gd interaction, one non-negligible 4f–4f overlap between two orbitals ( $f_{xz^2}$ – $f_{xz^2}$ ) have been detected and the  $S_{\text{ab}}$  values computed are *ca.* the same in both **1** and **2**. This indicates that the unpaired electron in the  $\pi_{\text{py}}^*$  orbital is not playing an important role in the Gd··Gd coupling (Note: similar  $J_2$  strength in **1** and **2**).

NBO analysis has been carried out to gain insight into the mechanism, which is charge transfer in nature (indirect). Quite interestingly, the  $\pi_{\text{py}}^*$  orbital is found to interact with the  $\delta$  type  $d_{xy}$  orbital (see Fig. S3 of the ESI†). This interaction is rather weak as revealed by the NBO second order-perturbation analysis. Besides, only a small increase in 5d occupation has been noted for **1** compared to **2** (0.48; 0.49 for **1** and 0.46; 0.46 for **2** for two Gd<sup>III</sup> atoms in each case). All this essentially indicates that the  $\pi_{\text{py}}^*$  orbital in **1** does not play a proactive role in the charge transfer mechanism. This suggests that the ferromagnetic contribution, which generally dominates in {3d–4f} pairs, is significantly weak in complex **1**. On the other hand, two  $\pi_{\text{py}}^*$ –4f interactions (see Fig. 2c–d) have been detected in the NBO second order perturbation analysis and this reinforces the significant  $\pi_{\text{py}}^*$ –4f-orbital interaction previously suggested from the overlap integral calculations.

The  $\pi_{\text{py}}^*$  orbital is strongly antibonding in character and has a large anionic charge, thus the lobes are very much diffused. This makes it ideal for overlap with 4f-orbitals and this interaction is very significant compared to any {3d–4f} pair computed earlier.<sup>13</sup> A significant  $\pi_{\text{py}}^*$ –4f-orbital interaction and a less significant charge transfer mechanism essentially lead to a very large antiferromagnetic  $J$  in **1**. Moreover, the {2p–4f} class of compounds enjoy close proximity to the lanthanide ions as the radical centres are directly coordinated to the metal ions. This essentially leads to significant direct interactions between the radical magnetic orbitals and the 4f-orbitals. On the other hand, in the {3d–4f} class, such overlap is super-exchange in nature, which eventually diminishes this contribution. Due to these mechanistic differences, the majority of the {3d–4f} complexes exhibit ferromagnetic coupling<sup>5d–g</sup> while the {2p–4f} class of compounds exhibit antiferromagnetic coupling. Although all the analysis has been performed on complex **1**, a similar trend has been noted for other {2p–4f} complexes calculated in Table 1. This suggests that the proposed mechanism of coupling is generic for a {2p–Gd<sup>III</sup>} class of compounds and we are confident that a similar mechanism is operational for the Ising type of exchange exhibited by other 4f-elements.

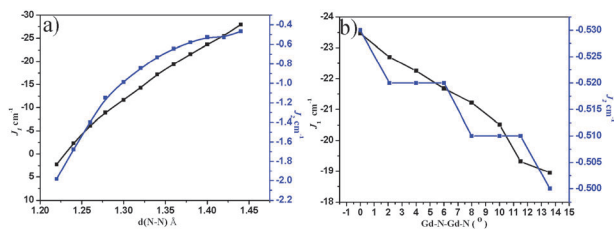


Fig. 3 Magneto structural correlations developed on complex 1.

We have developed some magneto-structural correlations on **1** to offer a way to enhance the magnitude of the  $J$  value. One of the large structural differences observed among the reported  $\{La_2N_2\}^{n+}$  core structures<sup>14</sup> are the N–N bond lengths of the bridging unit. The N–N length varies with respect to the charge of the  $N_2$  moiety and the ligand crowding surrounding the lanthanide ions. To underpin the effect of N–N distance on the magnetic coupling, the N–N distance was varied<sup>15</sup> from 1.40 Å to 1.22 Å in **1** and the developed correlation is shown in Fig. 3a. As the N–N distance increases, there is a considerable increase in  $J_1$  and  $J_2$  interactions. A rationale for this comes from the computed  $S_{ab}$  values, where a larger  $S_{ab}$  has been detected as the N–N length elongates (See Table S6 and S8 of the ESI†). Quite interestingly, below 1.278 Å, the interaction switches from antiferro to ferromagnetic. For the antiferromagnetic part, as the N–N distance elongates (compresses), the relative energy of the  $\pi_{py}^*$  orbital decreases (increases) and the net charge on the nitrogen atom increases (decreases) and this essentially leads to a strong (weak) Gd–radical interaction. The correlation essentially reveals that the N–N distance can be employed to fine tune the  $J$  values for this complex. Another parameter that is likely to influence the  $J$  value is the [N–Gd–N–Gd] dihedral angle. The developed correlation from varying the dihedral angle from 0° to 13.5° is shown in Fig. 3b (see ESI for details†). The interaction between  $J_1$  and  $J_2$  decreases as we increase the dihedral angle, suggesting that non-planarity of the  $\{Gd_2N_2\}$  unit weakens the exchange interaction. As the  $N_2^{3-}$  and  $Gd^{III}$  ions are twisted out of the plane, the overlap,  $S_{ab}$ , decreases as expected leading to decrease in the net exchange.

As per our knowledge, DFT calculations have been employed for the first time to model the  $J$  values of a  $\{2p-4f\}$  pair. Apart from obtaining good numerical estimates of  $J$  values, MO and NBO analysis have been employed to develop a generic mechanism of coupling for a  $\{2p-4f\}$  class of complexes. The radical magnetic orbitals are, in general, found to be diffused and interact strongly with the 4f orbitals of the lanthanide ions leading to large  $J$  values. This is contrary to the general belief that the 4f-orbitals are inert in nature. Besides, the regular  $3d \rightarrow Gd(5d)$  CT mechanism, which dominates the  $J$  values in the  $\{3d-4f\}$  class, is found to be weak in these complexes. To this end, our study indicates that radical bridging is an attractive alternate to the  $\{3d-4f\}$  class to achieve a strong exchange interaction. The magneto-structural correlations developed for **1** indicate that the longer N–N distance paves a way forward for strong exchange coupling in **1**.

GR would like to acknowledge financial support from DST India (SR/S1/IC-41/2010) and IIT Bombay for access to the high performance computing facility. TR acknowledges a JRF position from DST, India.

## Notes and references

- (a) R. Sessoli, D. Gatteschi, A. Caneschi and M. A. Novak, *Nature*, 1993, **365**, 141; (b) M. Leuenberger and D. Loss, *Nature*, 2001, **410**, 789.
- R. E. P. Winpenny, *J. Chem. Soc., Dalton Trans.*, 2002, 1.
- (a) S. Langly, N. Chilton, I. Gass, B. Moubaraki and K. Murray, *Dalton Trans.*, 2011, **40**, 12656; (b) B. H. Koo, K. S. Lim, D. W. Ryu, W. R. Lee, E. K. Koh and C. S. Hong, *Chem. Commun.*, 2012, **48**, 2519; (c) N. Ishikawa, M. Sugita, N. Ishikawa, S. -Y. Koshihara and Y. Kaizu, *J. Phys. Chem. B*, 2004, **108**, 11265; (d) N. Ishikawa, M. Sugita, T. Ishikawa, S.-Y. Koshihara and Y. Kaizu, *J. Am. Chem. Soc.*, 2003, **125**, 8694; (e) J. D. Rinehart, M. Fang, W. J. Evans and J. R. Long, *J. Am. Chem. Soc.*, 2011, **133**, 14236.
- (a) C. Benelli, A. Caneschi, D. Gatteschi, J. Laugier and P. Rey, *Angew. Chem., Int. Ed. Engl.*, 1987, **26**, 913; (b) A. Caneschi, A. Dei, D. Gatteschi, L. Sorace and K. Vostrikova, *Angew. Chem., Int. Ed.*, 2000, **39**, 246; (c) C. Lescop, D. Luneau, P. Rey, G. Bussiere and C. Reber, *Inorg. Chem.*, 2002, **41**, 5566; (d) C. Lescop, E. Belorizky, D. Luneau and P. Rey, *Inorg. Chem.*, 2002, **41**, 3375; (e) T. Tsukuda, T. Suzuki and S. Kaizaki, *J. Chem. Soc., Dalton Trans.*, 2002, 1721; (f) L. Norel, L.-M. Chamoreau, Y. Journaux, O. Oms, G. Chastanet and C. Train, *Chem. Commun.*, 2009, 2381; (g) H. Zhao, M. J. Bazile, J. R. Galan-Mascaros and K. R. Dunbar, *Angew. Chem., Int. Ed.*, 2003, **42**, 1015; (h) J. W. Raebiger and J. S. Miller, *Inorg. Chem.*, 2002, **41**, 3308.
- (a) R. Sessoli and A. K. Powell, *Coord. Chem. Rev.*, 2009, **253**, 2328; (b) C. A. Barta, S. R. Bayly, P. W. Read, B. O. Patrick, R. C. Thompson and C. Orvig, *Inorg. Chem.*, 2008, **47**, 2294; (c) J. Rinck, G. Novitchi, W. V. D. Heuvel, L. Ungur, Y. Lan, W. Wernsdorfer, C. E. Anson, L. F. Chibotaru and A. K. Powell, *Angew. Chem., Int. Ed.*, 2010, **49**, 7583; (d) J. -P. Costes, J. M. Clemente-Juan, F. Dahan, F. Dumestre and J.-P. Tuchagues, *Inorg. Chem.*, 2002, **41**, 2886; (e) S. Igarashi, S. -I. Kawaguchi, Y. Yukawa, F. Tuna and R. E. P. Winpenny, *Dalton Trans.*, 2009, 3140; (f) J. -P. Costes, F. Dahan and J. Garcia-Tojal, *Chem.–Eur. J.*, 2002, **8**, 5430; (g) F. Cimpoesu, F. Dahan, S. Ladeira, M. Ferbinteau and J.-P. Costes, *Inorg. Chem.*, DOI: 10.1021/ic3001784; (h) A. Mishra, W. Wernsdorfer, K. A. Abboud and G. Christou, *J. Am. Chem. Soc.*, 2004, **126**, 15648; (i) A. N. Georgopoulou, R. Adam, C. P. Raptopoulou, V. Psycharis, R. Ballesteros, B. Abarca and A. K. Boudalis, *Dalton Trans.*, 2010, **39**, 5020; (j) T. N. Hooper, J. Schnack, S. Piligkos, M. Evangelisti and E. K. Brechin, *Angew. Chem., Int. Ed.*, 2012, **51**, 4633; (k) S. Langly, L. Ungur, N. Chilton, B. Moubaraki, L. F. Chibotaru and K. S. Murray, *Chem. Eur. J.*, 2011, **17**, 9201.
- R. J. Blagg, C. A. Muryn, E. J. L. McInnes, F. Tuna and R. E. P. Winpenny, *Angew. Chem., Int. Ed.*, 2011, **50**, 6530.
- (a) K. C. Mondal, G. E. Kostakis, Y. Lan, W. Wernsdorfer, C. E. Anson and A. K. Powell, *Inorg. Chem.*, 2011, **50**, 11604; (b) A. Saha, M. Thompson, K. A. Abboud, W. Wernsdorfer and G. Christou, *Inorg. Chem.*, 2011, **50**, 10476.
- Y.-N. Guo, G.-F. Xu, W. Wernsdorfer, L. Ungur, Y. Guo, J. Tang, H.-J. Zhang, L. F. Chibotaru and A. K. Powell, *J. Am. Chem. Soc.*, 2011, **133**, 11948.
- J. D. Rinehart, M. Fang, W. J. Evans and J. R. Long, *Nat. Chem.*, 2011, **3**, 538.
- W. J. Evans, D. S. Lee, D. B. Rego, J. M. Perotti, S. A. Kozimor, E. K. Moore and J. W. Ziller, *J. Am. Chem. Soc.*, 2004, **126**, 14574.
- E. Ruiz, S. Alvarez, A. Rodriguez-Fortea, P. Alemany, Y. Pouillon and C. Massobrio in *Magnetism: Molecules to Materials*, ed. J. S. Miller and M. Drillon, Wiley-VCH, Weinheim, 2001, vol. II, p. 227; A. Bencini and F. Totti, *Int. J. Quantum Chem.*, 2005, **6**, 819; G. Rajaraman, M. Murugesu, E. C. Sanudo, M. Soler, W. Wernsdorfer, M. Helliwell, C. Muryn, J. Raftery, S. J. Teat, G. Christou and E. K. Brechin, *J. Am. Chem. Soc.*, 2004, **126**, 15445.
- Note: treating the two  $J_1$  interactions in **1** differently leads to  $J_{1a} = -23.8 \text{ cm}^{-1}$  and  $J_{1b} = -23.5 \text{ cm}^{-1}$ .
- (a) G. Rajaraman, F. Totti, A. Bencini, A. Caneschi, R. Sessoli and D. Gatteschi, *Dalton Trans.*, 2009, **17**, 3153; (b) S. K. Singh, N. K. Tibrewal and G. Rajaraman, *Dalton Trans.*, 2011, **40**, 10897.
- (a) W. J. Evans, G. Zucchi and J. W. Ziller, *J. Am. Chem. Soc.*, 2003, **125**, 10; (b) W. J. Evans, M. Fang, G. Zucchi, F. Furche, J. W. Ziller, R. M. Hoekstra and J. I. Zink, *J. Am. Chem. Soc.*, 2009, **131**, 11195; (c) M. Fang, J. E. Bates, S. E. Lorenz, D. S. Lee, D. B. Rego, J. W. Ziller, F. Furche and W. J. Evans, *Inorg. Chem.*, 2011, **50**, 1459.
- Note here that modifying the N–N distance also leads to very small changes in other geometrical parameters such as Gd–N distance and Gd–N–Gd angles.